

# Study on Mechanical Properties, Optical Properties, Cytotoxicity of TiO<sub>2</sub>-HAP Nanoparticles-Modified PMMA and Photodynamically Assisted Antibacterial Activity Against *Candida Albicans* in Vitro

Yubo Liu<sup>1,2</sup>, Zhongke Wang<sup>1,2</sup>, Xiangrui Liu<sup>1,2</sup>, Hongmei Chen<sup>1,2</sup>, Ying Huang<sup>1,2</sup>, Aodi Li<sup>1,2</sup>, Yifan Pu<sup>1,2</sup>, Ling Guo<sup>1,2</sup>

<sup>1</sup>Department of Oral Prosthodontics, The Affiliated Stomatological Hospital, Southwest Medical University, Luzhou, People's Republic of China;

<sup>2</sup>Luzhou Key Laboratory of Oral & Maxillofacial Reconstruction and Regeneration, Luzhou, People's Republic of China

Correspondence: Ling Guo, Department of Oral Prosthodontics, The Affiliated Stomatological Hospital, Southwest Medical University, Luzhou, People's Republic of China, Tel +86-15892900789, Email gsmiling@swmu.edu.cn

**Statement of Problem:** The high recurrence rate of denture stomatitis may be related to the strong resistance of fungi. Therefore, the method of providing biomaterials with antifungal properties is an attractive solution for improving microbial control.

**Purpose:** Against the drug resistance of *Candida albicans*, this study aim to elucidate the photocatalytic antibacterial effect of TiO<sub>2</sub>-HAP nanocomposite-modified PMMA on *Candida albicans* through in vitro experiments, and to evaluate the potential impact of the mechanical properties, optical properties, cytotoxicity and contact angle of the modified PMMA, to provide a scientific basis for the development of denture base resins with minimum percentage of photocatalytic additives.

**Methods:** In this study, TiO<sub>2</sub>-HAP nanoparticles were mixed with self-polymerized PMMA in different mass ratios, 0%wt was the control group. Various methods were used to characterize TiO<sub>2</sub>-HAP. Subsequently, the changes in mechanical and optical properties of the samples were measured, and Cell Counting Kit-8 (CCK-8) and cell live-death staining were used to detect the cytotoxicity of the samples to human gingival fibroblasts (HGFs) in vitro. The contact angle of the specimens was evaluated. The photocatalytic antibacterial activity of modified PMMA against *Candida albicans* was studied using a biofilm accumulation test and scanning electron microscopy.

**Results:** TiO<sub>2</sub>-HAP nanocomposites have an acceptable structure. When the addition amount of TiO<sub>2</sub>-HAP is 1.0%wt, the PMMA material showed peak mechanical properties. When the additional amount is less than 1%wt, The patient is still aesthetically acceptable PMMA showed no significant cytotoxicity at doses below 2%wt. While TiO<sub>2</sub>-HAP modified PMMA containing only 1%wt showed up to 94% antibacterial efficiency against *Candida albicans* under visible light.

**Conclusion:** Therefore, it is inferred that the optimal photocatalytic antimicrobial and mechanical properties of PMMA materials are achieved by adding 1%wt TiO<sub>2</sub>-HAP without causing significant changes in cytotoxicity and optical properties.

**Keywords:** TiO<sub>2</sub>-HAP, polymethyl methacrylate, photodynamic therapy, *Candida albicans*, antibiofilm

## Introduction

Dentition deflection and loss are highly prevalent conditions globally, Epidemiological evidence shows that 2.3% of the world's population has complete edentulism.<sup>1</sup> Dentition deflection and loss may occur at any age, but geriatric patients have the highest prevalence.<sup>2</sup> For elderly patients, the preferred treatment option is the removable denture, because it is inexpensive and can be cleaned easily, When the teeth are lost further, the removable denture can add teeth easier.<sup>3</sup> Currently, polymethyl methacrylate (PMMA) is an important part of the denture, it has many advantages such as superior biocompatibility, aesthetics, inexpensiveness, stability, and processability.<sup>4</sup> In addition to being the main material for the denture, it can also be used to fabricate maxillofacial prostheses, oral orthodontic appliances, occlusal splints, artificial

teeth, etc.<sup>5,6</sup> However, its mechanical properties are poor, it is very easy to break during use.<sup>7</sup> In the face of a complex oral environment, pure PMMA lacks antimicrobial properties, and if poorly cleaned, it may lead to a large number of pathogenic bacteria colonization, increasing the risk of suffering from denture stomatitis and other infectious diseases.<sup>8</sup> Among denture wearers, the incidence of denture stomatitis (DS) is as high as 70%.<sup>9</sup> DS is a chronic disease of the oral mucosa, the mucosa of the denture-bearing area becomes red and swollen and appears yellow and white pseudomembrane.<sup>10</sup> *Candida albicans* (*C. Albicans*) is one of the common microorganisms in a healthy oral cavity, however, under certain conditions, it can become pathogenic.<sup>11</sup> Adhesion of *C. Albicans* and biofilm formation on the surface of the resin base is closely associated with DS.<sup>12</sup>

Currently, traditional methods to reduce the amount of biofilm on the surface of PMMA Denture Base include mechanical cleaning and chemical soaking, but they may damage the denture's physical properties, increase surface roughness, change color, etc.<sup>13</sup> In recent years, in response to the drug resistance to *Candida albicans*, scholars have developed an effective treatment strategy - photodynamic therapy (PDT). Its antibacterial principle is that under aerobic conditions, photosensitizers are added to tissues or outside living cells, and activated by light of specific wavelengths to produce reactive oxygen species and attack microorganisms.<sup>14</sup> PDT does not produce drug resistance, Even for repeated infections caused by drug-resistant *C. Albicans*, it still works well.<sup>15</sup>

Titanium dioxide ( $\text{TiO}_2$ ) nanoparticles have shown great potential as an antibacterial material due to its unique photocatalytic activity. It has excellent biocompatibility, chemical stability, and corrosion resistance.<sup>16</sup> It can be used as an ideal photocatalyst and photosensitizer. Under ultraviolet (UV) irradiation, it can form electron-hole pairs, which then interact with  $\text{O}_2$  and  $\text{OH}^-$  to form superoxides and free hydroxyl radicals ( $\cdot\text{OH}$ ), which then damage bacteria and kill cells.<sup>17</sup>  $\text{TiO}_2$  nanoparticles have been extensively used in the field of denture restoration in recent years, and by incorporating antibacterial agents into the PMMA denture base, researchers have enhanced the material's mechanical and antibacterial qualities.<sup>18,19</sup> Its primary drawbacks, however, are that photogenerated electron-hole pairs recombine quickly and that it is only activated by ultraviolet light, which restricts its use in routine clinical practice.<sup>20</sup> The development of  $\text{TiO}_2$ -based materials that can maximize visible light use, improve photocatalytic activity, and produce effective bactericidal effects is crucial.

Hydroxyapatite (HAP) nanoparticles are a kind of calcium phosphate material, and it is an important component of bone and teeth, it is easy to obtain and has good biological activity. It has been applied in many fields.<sup>21</sup> It has been shown that HAP can improve the photocatalytic efficiency and broaden the photoresponse range of  $\text{TiO}_2$ .<sup>22</sup> In addition, HAP can also be used as an inorganic filler to increase the mechanical properties of the PMMA base.<sup>23</sup>

There have been studies with nanoparticles synthesized by simple methods and shown excellent antimicrobial and photocatalytic properties.<sup>24</sup> Despite these advances, research with nanoparticle nanoparticles on the role of  $\text{TiO}_2$ -HAP nanoparticles in PMMA materials, In particular, studies on its antimicrobial and mechanical properties are still limited, suggesting that this is a ripe area for further research. When designing new materials for dental use, all the parameters studied are important, though often overlooked. Therefore, the main objective of the ex vivo study is to evaluate the photocatalytic antifungal effect of PMMA modified with  $\text{TiO}_2$ -HAP nanoparticles. The mechanical properties, optical properties, cytotoxicity, and contact angle of the modified resin were also evaluated. To test these objectives, we formulated the following null hypothesis: 1) visible-activated  $\text{TiO}_2$ -HAP modified PMMA has no inhibitory activity against *Candida albicans*. 2)  $\text{TiO}_2$ -HAP does not cause any significant changes in the mechanical strength, optical properties, cytotoxicity, or contact angle of PMMA.

## Materials and Methods

### Materials

$\text{TiO}_2$  nanoparticles and Ammonia (25–28%) were purchased from Shanghai Macklin Biochemical Technology Co., Ltd., China. HAP (Hangzhou Shark Biotechnology Co., Ltd., China); Self-curing PMMA denture base resin (including liquid and powder, Shanghai Eryi Zhangjiang Biomaterial Co., Ltd., China).

### Preparation and Characterization of $\text{TiO}_2$ -HAP Nanoparticles

Hydroxyapatite nanoparticles were dissolved in 0.1 mol/L HCl, and then nano- $\text{TiO}_2$  suspensions were added. The molar ratio between HAP and  $\text{TiO}_2$  was 2:1. To modify the pH to 11–12, add ammonia water to the solution. The solution was

agitated and heated at 90°C for 6 hours. The sediment is filtered and rinsed three times with distilled water. The sample was dried at 80°C in a vacuum dryer (DZF-6020, Shaoxing Supo Instrument Co., Ltd., China) to produce TiO<sub>2</sub>-HAP powder. Fourier transform infrared spectroscopy (Jasco, 6300, Tokyo, Japan) was used to record the infrared spectra of powder samples dispersed on KBr plates, while SEM (Inspect F50, Thermo Fisher, USA) and HRTEM (JEM-2100) were used to record the infrared spectra of powder samples dispersed on KBr plates. Japan) evaluated the surface morphology of the samples; EDS (EDS, AMETEK, USA) determined element composition; and XRD (D8 advance, NASDAQ: BRKR, USA) was utilized to analyze the materials' structural properties and identify crystalline phases. The optical characteristics of the sample were evaluated using a UV-vis spectrophotometer.

## Preparation of Polymethyl Methacrylate (PMMA)-Based Dental Resin Specimens Containing TiO<sub>2</sub>-HAP

TiO<sub>2</sub>-HAP was added to the base powder of a self-curing denture at 0:100, 0.5:100, 1:100, 1.5:100, and 2:100 (mass ratio to base powder), respectively, using a ball mill (GT300, Beijing Grinder Instrument Co., Ltd., China), mixed well, and then mixed evenly according to the manufacturer's instructions using a weight ratio of powder to liquid of 2:1. An appropriate amount was placed in the groove of the silicone mold. After the specimen had dried for 30 minutes, the surface was polished with sandpaper until the upper and lower surfaces were parallel and smooth. The specimen was then immersed in aqueous ethanol for 30 minutes, washed with sterile PBS, and dried naturally before being exposed to UV irradiation for 24 hours to sterilize.

## Measurement of Tensile Strength

Dumbbell-shaped specimens with a total length of 75mm, center width of 4mm, and overall thickness of 2.5mm were created. The tensile strength was measured using an electronic universal testing machine (INSTRON, 5965, Massachusetts, USA) with a uniform span of 55mm. The crosshead speed was adjusted to 5mm min<sup>-1</sup>, and the tensile strength was calculated based on the fracture of the specimen.

## Measurement of Flexural Strength and Flexural Modulus

To conduct a three-point flexural experiment, prepare 60mm×10mm×2.5mm cuboid samples and use an electronic universal testing machine (INSTRON, 5965, Massachusetts, United States) with a 50mm fulcrum span on both sides. The crosshead speed was adjusted to 5mm min<sup>-1</sup>, and the flexural strength and flexural modulus were calculated based on the fracture of the specimen.

## Optical Properties Evaluation

Under the same background, the transparency of each group of samples was measured using a transmittance detector (Linshang Technology, Shenzhen, China). The color difference was assessed using the CIE colorimetric method.<sup>25</sup> Three parameters define color in this system: L\*a\*and b\*representing lightness, redness-greenness, and yellowness-blueness, respectively. Where redness is +a\* and greenness is -a\*while yellowness is represented by +b\* and blueness by -b\*.<sup>25</sup> The change of sample color ( $\Delta E$ ) was calculated by the formula:

$$\Delta E = [(\Delta L^*)^2 + (\Delta a^*)^2 + (\Delta b^*)^2]^{1/2}$$

$\Delta L^*$ ,  $\Delta a^*$  and  $\Delta b^*$  represent the difference of L, a, and b values between each experimental group and the control group, respectively. The National Bureau of Standards (NBS) was used to quantify the level of  $\Delta E$  (Table 1) according to the following formula:

$$\text{NBS unit} = \Delta E \times 0.92$$

## Cytotoxicity Assay

Human gingival fibroblasts (HGFs) were received from the Oral & Maxillofacial Reconstruction and Regeneration of Key Laboratory, and their identification was completed in earlier studies by our study group.<sup>26</sup> The cell media was

**Table 1** Critical Marks of Color Difference According to the National Bureau of Standards (NBS)

NBS units	Clinical Interpretation
0.0–0.5	Trace
0.5–1.5	Slight
1.5–3.0	Noticeable
3.0–6.0	Appreciable
6.0–12.0	Much

DMEM containing 10% FBS (fetal bovine serum) and antibiotics. Thermo Fisher Scientific Inc. provided all media and reagents for cell experiments, while Dojindo Laboratories provided the Cell Counting Kit-8 (CCK-8) assay kit.

We evaluated the cytotoxicity of the materials according to ISO standard 10993–12:200 guidelines. Following sterilization, samples from each group were immersed in DMEM medium for one week, and each group extracted 1 mL. The final extract was then prepared by adding 10% FBS and 1% double antibody and refrigerating the extract at 4°C for future use. HGFs were grown in a full medium at 37°C and 5% CO<sub>2</sub> for logarithmic growth. Cells were placed in 96-well plates at a density of 5×10<sup>3</sup> cells/well and cultivated for 24 hours. After 24 hours, the original culture media was withdrawn from the holes, washed twice with PBS, and 100µL extract was reintroduced to each group sequentially for further culture. After 24 hours, 48 hours, and 72 hours, the extract was removed and replaced with 10µL CCK-8 solution and 100µL of complete culture media. The absorbance (OD) value was measured at 450 nm using SynergyH1, BioTek, USA. Each experiment was repeated three times.

At the same time, each group's HGFs were stained with a Calcein AM/PI live and dead cell double staining kit (Elabscience Biotechnology Co., Ltd., Wuhan, China) after 24 hours, 48 hours, and 72 hours of culture. The stained cells were examined using an inverted fluorescent microscope (Zeiss LSM 700, Germany).

## Contact Angle Measurements

The site-drop method was used to examine the specimens' contact angle. From each group, three samples were chosen, and five microliters of deionized water droplets were applied to their surface at room temperature. Using a contact angle measuring device (KRUSS, DSA25, Germany), the water contact angle is determined and recorded.

## Bacterial Recovery and Culture

Luzhou Keyang Biotechnology Co., Ltd Provided *Candida albicans* standard strain (CMCC (F) 98001), as well as culture media and reagents for bacterial experiments. The glycerin-frozen bacteria were removed from the refrigerator at –80°C, melted, and mixed with the Salle liquid medium, and the bacterial solution was resuscitated on the Salle solid culture using the inoculation ring. The culture dish was incubated at 37°C for 24 h, and a colony was selected in Salle liquid medium, incubated in the incubator at 37°C for 12 h, and diluted to the required concentration for subsequent experiments.

## Antifungal Properties

The antimicrobial activity of the surface of the material was evaluated using the biofilm accumulation test of ISO 22196:2011.<sup>27</sup> We chose the 1%wt TiO<sub>2</sub>-HAP specimen for further testing and made PMMA specimens with only 1%wt TiO<sub>2</sub>. Samples of 0%wt TiO<sub>2</sub>-HAP, 1%wt TiO<sub>2</sub>-HAP, and 1%wt TiO<sub>2</sub> were put in 24-well plates. Each well received 2 mL of *Candida albicans* suspension at a concentration of 1×10<sup>7</sup> CFU mL<sup>-1</sup>. The light group was exposed to a dental curing lamp (385 nm–515 nm, woodpecker, X-cure, soft mode) for 15 minutes, with a distance of 0.5 cm between the lamp and the liquid surface. The specimen was then incubated at 37°C anaerobic for 24 hours before being gently washed

with PBS three times. Place it in a centrifuge tube with 2 mL PBS. After 5 minutes of centrifugation at 3000r, *Candida albicans* adhered to the surface of the PMMA specimen were removed. The suspension is diluted and plated on Sabouraud agar. After 24 hours of incubation at 37°C, count the colonies and determine the number of colony-forming units (CFU) per milliliter. Additionally, we used SEM to study the biofilm that had grown on the specimen surface. The specimens of each group were gently rinsed with PBS twice, submerged in a 2.5% glutaraldehyde solution, and fixed at 4°C overnight. The specimens were dehydrated in a gradient of 30%, 50%, 70%, 90%, and 100% ethanol for 15 minutes each, then dried using a vacuum freeze dryer (LABCONCO, USA) before being coated with gold. A scanning electron microscope (SEM, Quanta 650, ThermoFisher Scientific, Waltham, MA, USA) was used to examine *Candida albicans* on the specimen's surface.

## Statistical Analysis

SPSS 17.0 software was used for statistical analysis. All measurements in this study were independently repeated 3 times. One-way ANOVA (Duncan test) was performed to assess the differences between groups and analyze the significance of the data. The measurement data were expressed as mean±standard deviation ( $\bar{x} \pm s$ ) and plotted with Origin 2021 software.  $P < 0.05$  was considered to be statistically significant.

## Results

### TiO<sub>2</sub>-HAP Characterization

According to the SEM image in Figure 1A, the morphology of the TiO<sub>2</sub>/HAP nanocomposite was shown, and the composite showed a porous cluster structure. The energy dispersive X-ray (EDX) spectra and element mapping (Figure 1B) show that TiO<sub>2</sub> is uniformly located on the surface of HAP, revealing the uniform distribution of Ti, Ca, and P. FTIR spectra are shown in Figure 1C. The complex showed a strong broadband absorption peak at 3300–3600 cm<sup>-1</sup>, corresponding to the stretching vibration peaks of hydroxyl groups on the surface of TiO<sub>2</sub> and hydroxyl groups adsorbed in water, indicating that there were abundant hydroxyl groups on the surface of the obtained products, which could be inferred that the products had good photocatalytic activity.<sup>28</sup> The absorption peak between 500 and 800 cm<sup>-1</sup> is the vibration peak of Ti-O-Ti in the TiO<sub>2</sub> structure.<sup>29</sup> The peaks at 565 cm<sup>-1</sup>, 603 cm<sup>-1</sup>, 961 cm<sup>-1</sup>, 1033 cm<sup>-1</sup> and 1093 cm<sup>-1</sup> are the stretching and flexural movements of PO<sub>4</sub> groups.<sup>30</sup> The results obtained by X-ray powder diffraction analysis (Figure 1D) show that the crystal faces of (021), (302), (312) and (321) of brookite TiO<sub>2</sub> (JCPDS card 72-0100) and (1 12), (130), (1 32) and (5) of HAP (JCPDS No-74-0565)

According to the HRTEM image (Figure 1E), the TiO<sub>2</sub> / HAP composite is a nanoparticle with a particle size of about 20 nm. The (021) crystal face of TiO<sub>2</sub> crystal and the (210) crystal face of HAP crystal were observed. The corresponding characteristic electron diffraction ring further determines the phase structure, which is consistent with the results of XRD characterization. These results indicate that the synthesis of TiO<sub>2</sub>-HAP is successful.

### Photocatalytic Activity

The catalytic activity of photocatalyst mainly depends on the light absorption capacity and band gap.<sup>31</sup> Figure 2A shows the UV-vis diffuse reflectance spectra (UV-vis DRS) of TiO<sub>2</sub>, HAP, and TiO<sub>2</sub>-HAP complexes. Due to the loading of HAP particles, TiO<sub>2</sub>-HAP exhibits higher absorption efficiency in the visible light range (400nm-700nm) than TiO<sub>2</sub> or HAP alone. Nanocomposites exhibit absorption redshift ( $\lambda > 390$  nm) and obtain band gap energy through the UV-Vis absorption spectrum. As shown in Figure 2B, the band gap value of the TiO<sub>2</sub>-HAP composite sample is 3.07eV and that of TiO<sub>2</sub> is 3.2eV. Therefore, the introduction of HAP broadened the spectral response range of TiO<sub>2</sub>. The weak photocatalytic ability of TiO<sub>2</sub> in the visible region is improved, to generate more hydroxyl radicals and enhance the antibacterial effect.

### Mechanical Properties

The experimental results are shown in Figure 3. The tensile strength, flexural strength, and flexural modulus of PMMA specimens in the experimental group showed a trend of first increasing and then decreasing with the increase of the addition



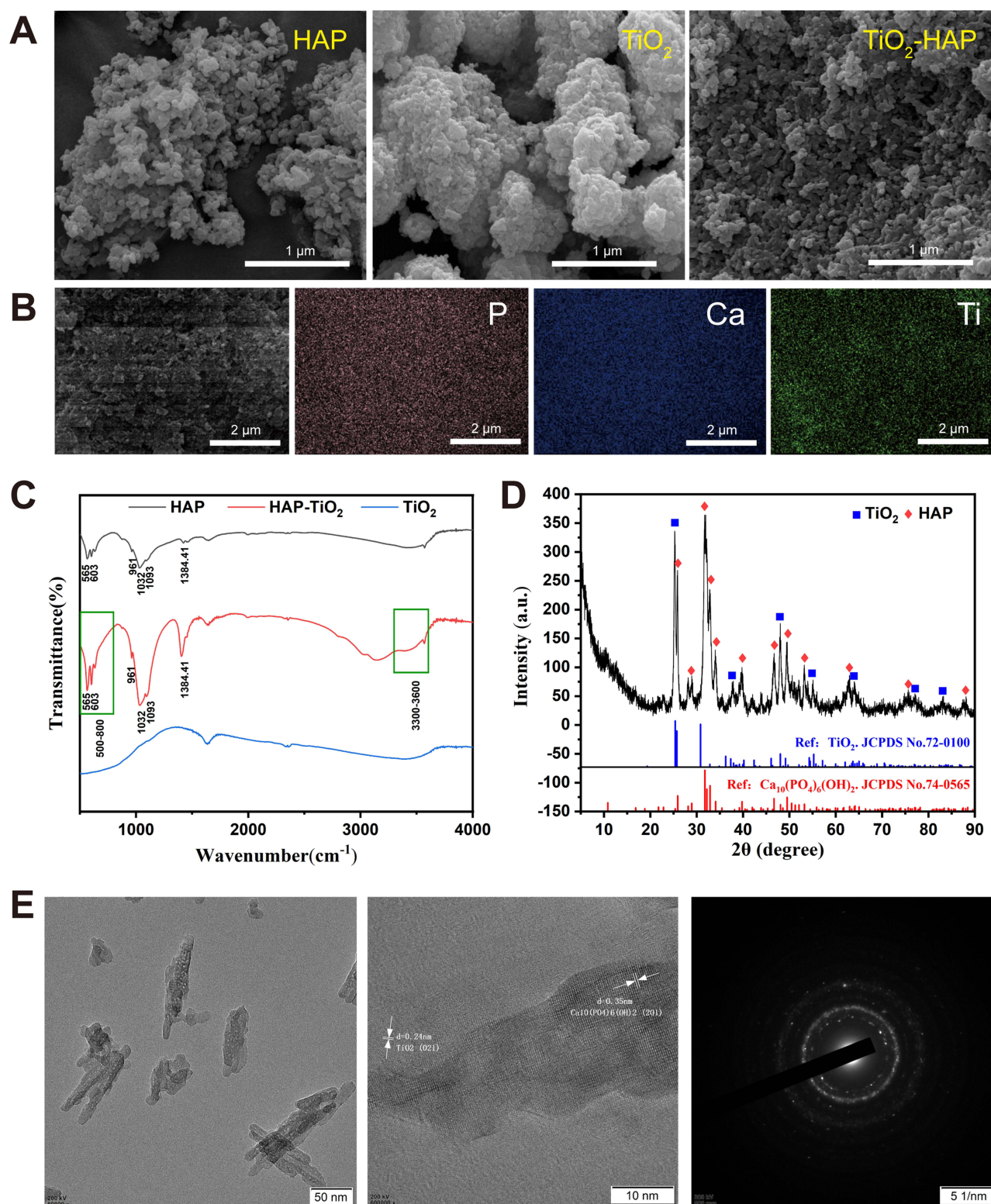


**Figure 1** Characterization of  $\text{TiO}_2$ -HAP nanocomposite. (A) SEM image. (B) Element mapping images for P, Ca and Ti. (C) IR spectrum. (D) XRD pattern. (E) HRTEM image.

proportion. When the content of the compound was 1%wt, the tensile strength, flexural strength, and flexural modulus of the PMMA base reached the maximum value. This indicates that the addition of  $\text{TiO}_2$ -HAP can enhance the different mechanical properties of PMMA base materials, and the enhancement effect is best when the addition ratio is 1%wt.

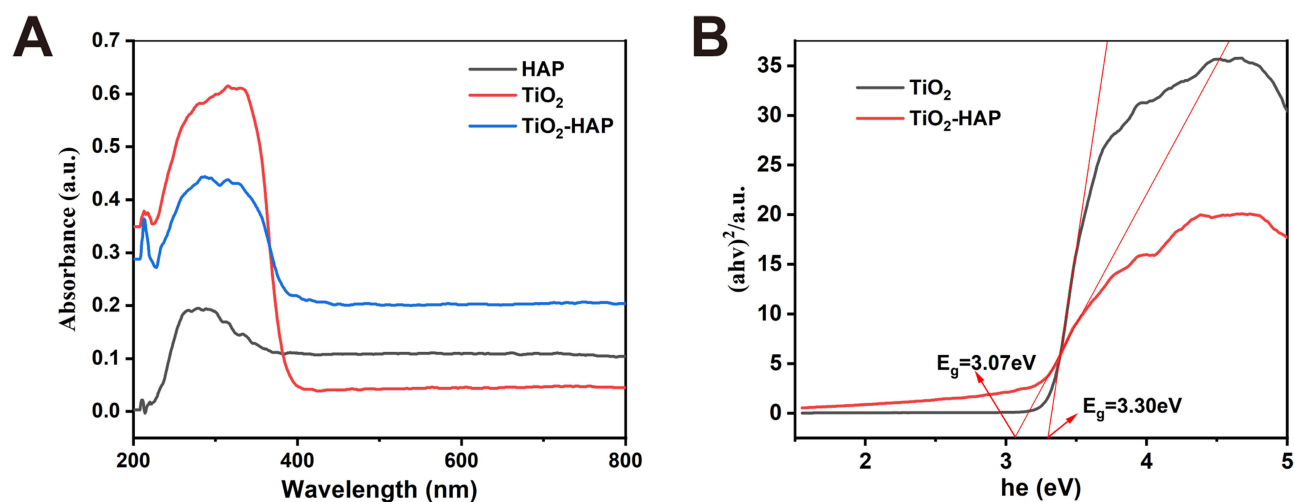


**Figure 2** (A) Absorbance UV/vis spectra of TiO<sub>2</sub>, HAP, and TiO<sub>2</sub>-HAP nanocomplexes. (B) Determination of the band gap energy values for TiO<sub>2</sub> and TiO<sub>2</sub>-HAP nanoparticles.

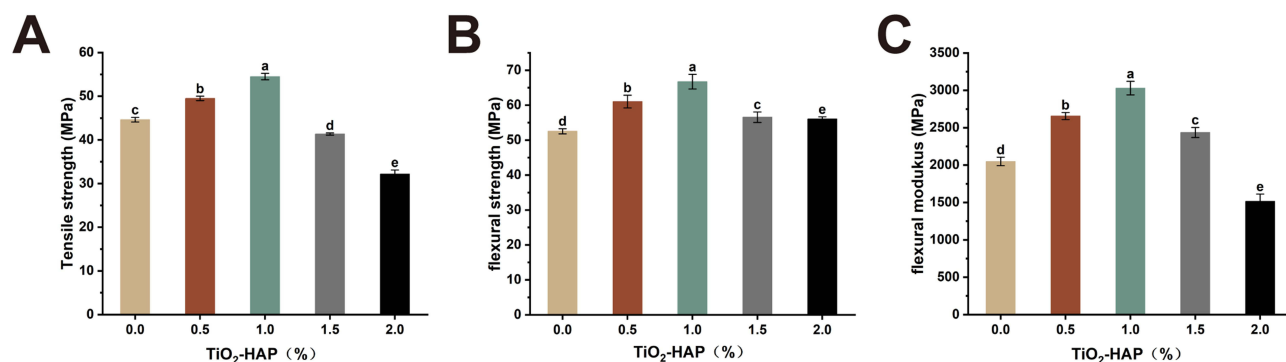


**Figure 3** Mechanical properties of TiO<sub>2</sub>-HAP composite specimens of different proportions. (A) Tensile strength. (B) Flexural strength. (C) Flexural modulus. Means indicated by different lowercase letters are significantly different ( $P < 0.05$ ). a, b, c, d, e < 0.001.

## Optical Properties Evaluation

The detection pictures of the transmittance of different groups (Figure 4A) show that: With the increase of the proportion of TiO<sub>2</sub>-HAP addition, the transmittance of the specimen gradually decreased. There were statistical differences in all groups ( $P < 0.05$ ). The  $l^*a^*$  and  $b^*$  parameters of the CIE color space are shown in Figure 4B, indicating that the addition of TiO<sub>2</sub>-HAP nanoparticles to PMMA increased the brightness and shifted the color to more green and blue. The  $l^*$  and  $a^*$  values of 0.5%wt and 1%wtPMMA samples showed no statistical difference compared with the control group ( $P > 0.05$ ). The  $l^*$  and  $a^*$  values of 1%wt and 1.5%wtPMMA specimens were statistically significant compared with those of the control group ( $P < 0.05$ ). The  $b^*$  values of 0.5%wt, 1%wt, and 1.5%wtPMMA specimens were not significantly different from those of the control group ( $P > 0.05$ ). The  $b^*$  value of the 2%wtPMMA specimen was significantly different from that of the control group ( $P < 0.05$ ). Based on the clinical threshold described by the National Bureau of Standards (NBS) (Table 1), according to the results in Table 2, the degree of color difference perception of people in the 0.5%wt group and the 1%wt group was slight (NBS 0.5 ~ 1.5). The color difference perception of the 1.5%wt group was noticeable (NBS 1.5~3.0). The color difference perception of the 2%wt group was very significant (NBS 6.0~12.0). In all experimental groups, only 0.5%wt and 1%wt of the groups had color changes within the clinically acceptable range.

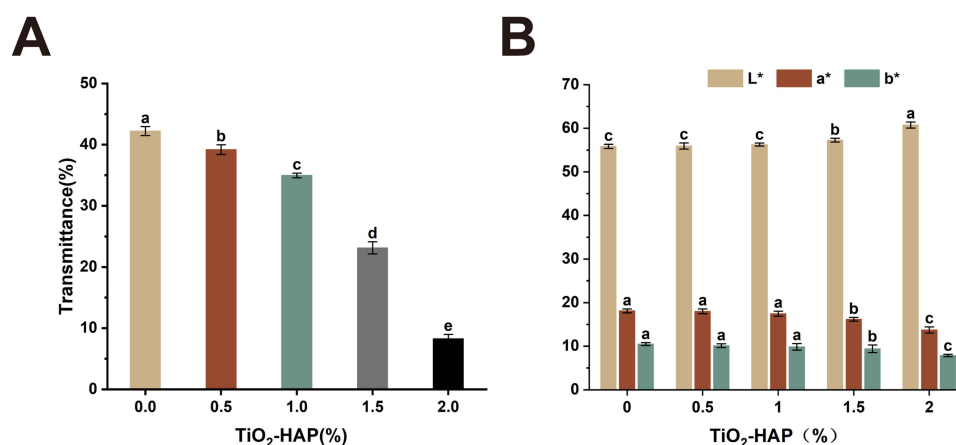


**Figure 4** Optical properties of TiO<sub>2</sub>-HAP composite PMMA specimens of different proportions. (A) transmittance. (B) CIE L\*a\*b\* parameters. Means indicated by different lowercase letters are significantly different. Means indicated by the same lowercase letter are not significantly different ( $P < 0.05$ ). a, b < 0.005, c, d, e, f < 0.001.

## Cytocompatibility Evaluation

As indicated in Figure 5A, OD values were taken at a wavelength of 450 nm following the co-cultivation of the aforementioned extracts with gingival fibroblasts for 24 hours, 48 hours, and 72 hours, respectively. When comparing the experimental groups to the blank group at 24, 48, and 72 hours, univariate analysis of variance (ANOVA) revealed no statistically significant differences ( $P > 0.05$ ). Meanwhile, the addition of TiO<sub>2</sub>-HAP also did not significantly limit cell proliferation, as demonstrated by cell survival staining (Figure 5B). The results show that the modified PMMA denture base resin has good biocompatibility.

## Contact Angle Measurement

We tested the wettability of PMMA after adding different proportions of TiO<sub>2</sub>-HAP nanoparticles using contact angle measurement (Figure 6). As the proportion of TiO<sub>2</sub>-HAP composites added increased, the contact angle of the specimen surface reduced, showing that the addition of TiO<sub>2</sub>-HAP composites improved the hydrophilicity of PMMA materials.

## Antibacterial Property

The antibacterial activity of titanium-hydroxyapatite nanoparticles doped PMMA samples against *Candida albicans* was investigated using the biofilm accumulation test, as illustrated in Figure 7A and B. Under no light conditions, there was no significant difference in bacterial inhibition rates between the TiO<sub>2</sub>-HAP +LED and TiO<sub>2</sub>+LED groups. Under light conditions, the number of colonies in the TiO<sub>2</sub>-HAP +LED group and the TiO<sub>2</sub>+LED group reduced dramatically, with

**Table 2** Color Change ( $\Delta E$ ) Between Experimental Groups and Pure PMMA

Group	$\Delta E$
0.00%	
0.50%	0.87±0.22
1.00%	1.2±0.24
1.50%	2.48±0.35
2.00%	6.40±0.55



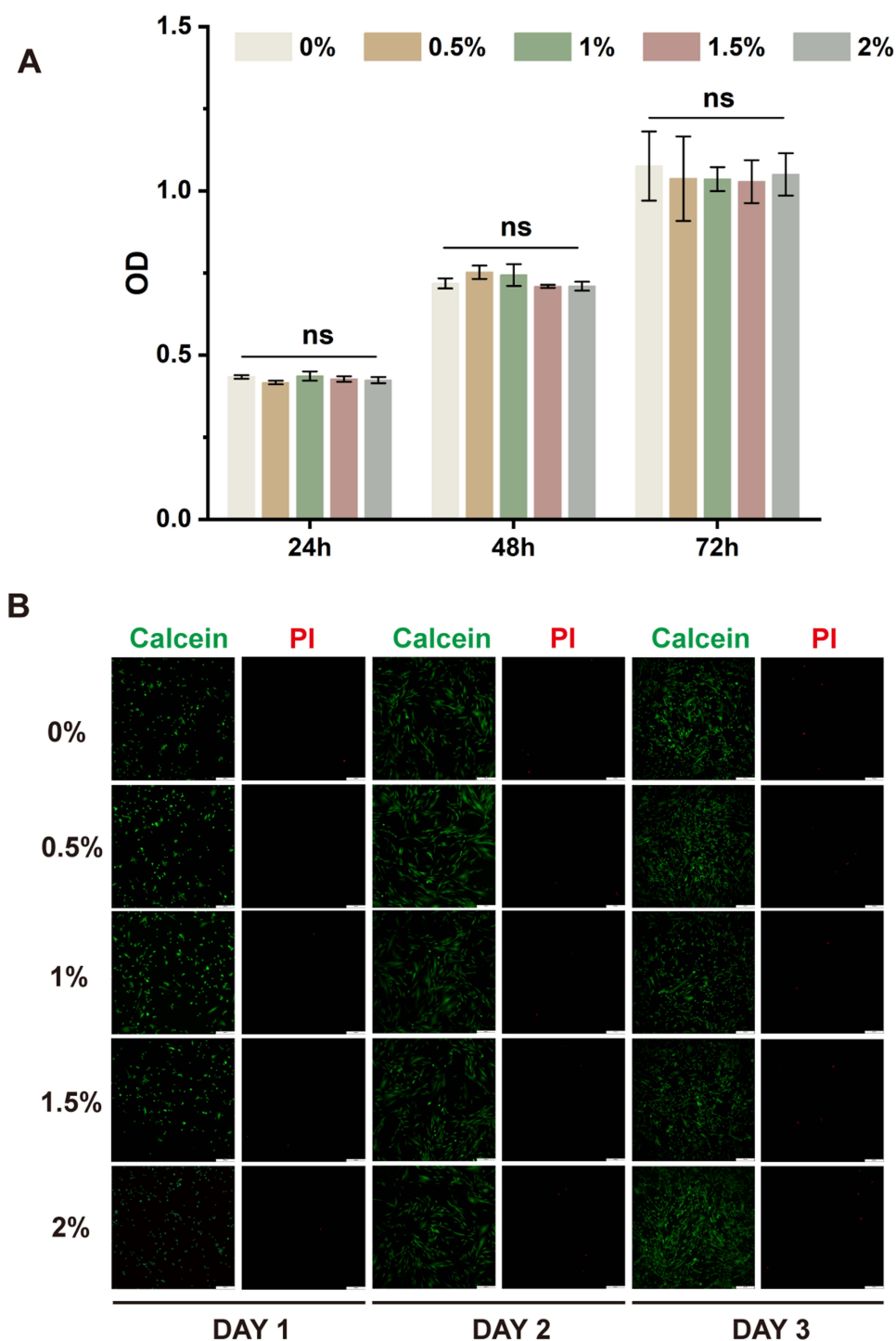


**Figure 5 (A)** The CCK-8 method was used to detect the effects of different proportions of TiO<sub>2</sub>-HAP composite PMMA specimens on cell proliferation activity. **(B)** Live and dead cell staining. (ns,  $P > 0.05$ ).

antibacterial rates of 94% and 86%, respectively. The results showed that HAP enhanced the antibacterial action of the modified PMMA in visible light compared to the PMMA doped with TiO<sub>2</sub>.

SEM images (Figure 7C) revealed that a large number of *Candida albicans* grew on the surface of the pure PMMA material with or without light irradiation, whereas only a few *Candida albicans* grew on the surface of the TiO<sub>2</sub>-HAP and pure TiO<sub>2</sub>-doped PMMA materials under blue light. Under visible light irradiation, the TiO<sub>2</sub>-HAP nanocomposite doped

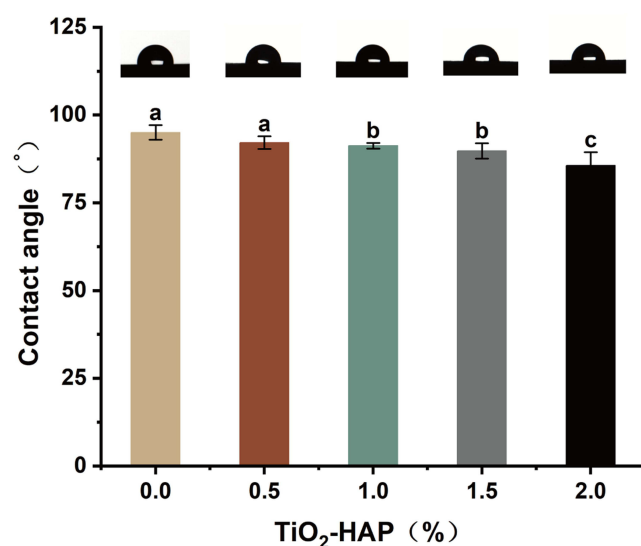


**Figure 6** Representative images of surface water droplets and corresponding contact angle values of TiO<sub>2</sub>-HAP composite PMMA specimens of different proportions. Means indicated by different lowercase letters are significantly different. Means indicated by the same lowercase letter are not significantly different ( $P < 0.05$ ). a,  $b < 0.005$ , c  $< 0.001$ .

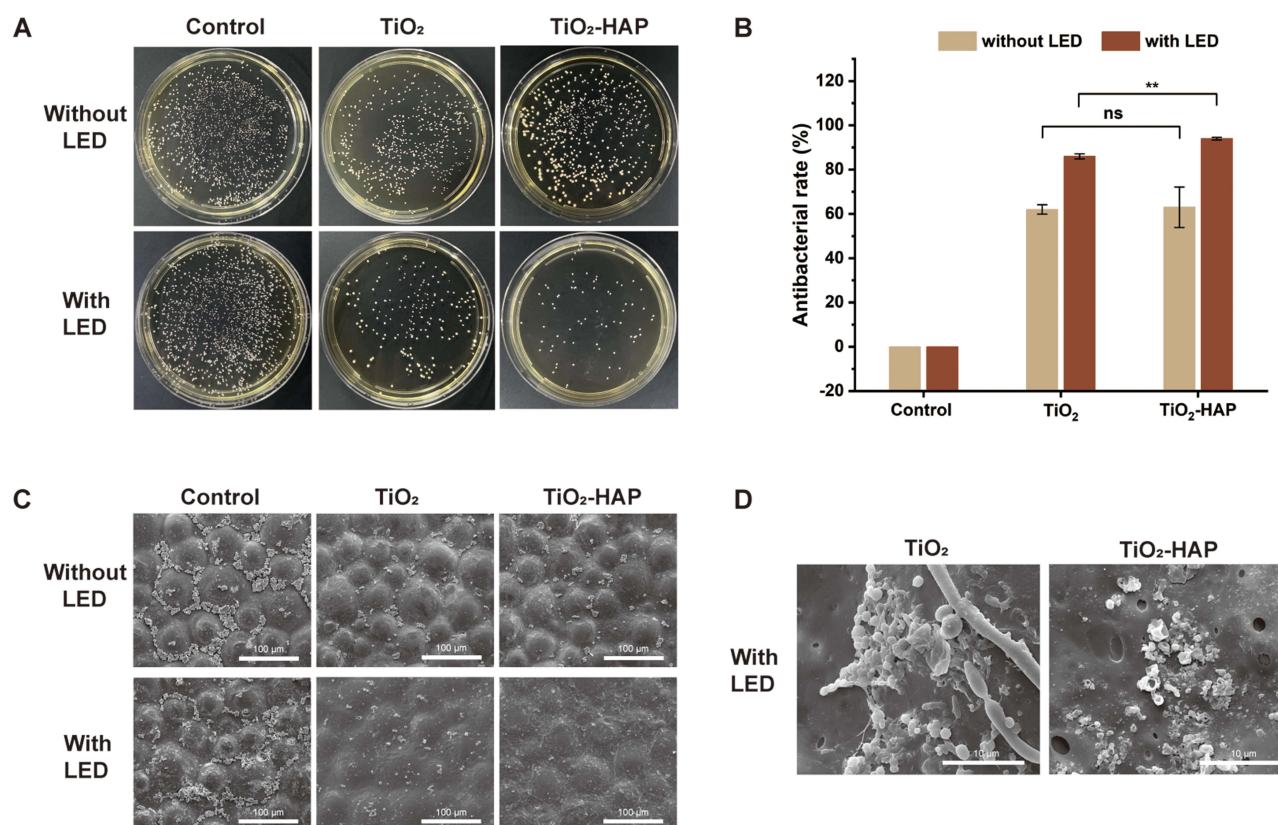


**Figure 7** Antibacterial activity of PMMA with 1%wtTiO<sub>2</sub> and 1%wtbrookite TiO<sub>2</sub>-HAP nanoparticles under visible and invisible light. (A) Antibacterial activity by the agar plate test. (B) Antimicrobial rate. (C) Scanning electron micrographs of PMMA surfaces in each group. (D) Enlarged scanning electron micrographs of PMMA surfaces. (ns,  $P > 0.05$ , \*\* $P < 0.01$ ).

PMMA material demonstrated improved anti-adhesion properties against *Candida albicans*. Consistent with the results of the agar plate antimicrobial test, the presence of germ tubes and mycelium could not be observed on the surface of modified PMMA under high magnification (Figure 7D), however, the fungal cells were ruptured and the contents were expelled after blue light irradiation. Overall, the improved PMMA material was more effective in inhibiting the fungus.

## Discussion

This study aims to clarify the photocatalytic antibacterial effect of TiO<sub>2</sub>-HAP nanocomposites-modified PMMA on *Candida albicans* through in vitro experiments, and to evaluate the potential impact of TiO<sub>2</sub>-HAP on the mechanical properties, optical properties, cytotoxicity, and contact angle of PMMA. Development of denture base resins with a minimum percentage of photocatalytic additives. Contrary to the null hypothesis that visible light-activated TiO<sub>2</sub>-HAP-modified PMMA has no inhibitory activity against *Candida albicans*, the results show that this hypothesis is rejected. In contrast, acceptance of the null hypothesis indicates that TiO<sub>2</sub>-HAP does not adversely affect the mechanical strength, optical properties, cytotoxicity, and contact angle of PMMA.

TiO<sub>2</sub> is a potential photocatalyst material and an effective antibacterial agent, it has antibacterial and antimicrobial properties through the production of oxygen free radicals, which can destroy the cell wall of certain bacteria and inhibit the formation of biofilms.<sup>32</sup> HAP is a type of catalyst-supporting substrate with excellent adsorption and photocatalytic characteristics, and it may work with metal catalysts to increase the photocatalytic properties of composite materials.<sup>33</sup> In this study, we successfully synthesized TiO<sub>2</sub>-HAP nanoparticles, and electron microscopy showed that the surface of HAP particles was uneven, with spherical particles uniformly attached to them to form TiO<sub>2</sub>-HAP composite phases with sizes ranging from about tens of nanometres to hundreds of nanometres, and interestingly, the XRD results of the materials showed that the attached TiO<sub>2</sub> nanoparticles were brookite TiO<sub>2</sub> (JCPDS card 72-0100), which is inconsistent with the result in some studies where TiO<sub>2</sub> in TiO<sub>2</sub>/HAP complexes is mainly anatase TiO<sub>2</sub> (JCPDS card 75-1537).<sup>22, 24</sup> Whereas in our study, anatase TiO<sub>2</sub> was converted to brookite TiO<sub>2</sub>, and this conversion may be due to the special hydrothermal conditions during the synthesis, which was explained in Keesmann's study.<sup>34</sup> Theoretical studies in recent years have shown that the brookite crystal phase has better photocatalytic performance than anatase and rutile due to its unique trapezohedron structure.<sup>20</sup> And this may provide a new idea for the application of brookite TiO<sub>2</sub>. UV-vis diffuse reflection spectroscopy (UV-vis DRS) revealed that TiO<sub>2</sub>-HAP has a greater absorption efficiency than TiO<sub>2</sub> or HAP alone in the visible region (400nm-700nm). Meanwhile, the band gaps of TiO<sub>2</sub>-HAP and TiO<sub>2</sub> have been determined to be 3.07 eV and 3.2 eV, respectively (Figure 2B), showing that HAP doping in TiO<sub>2</sub> can minimize the band gap of TiO<sub>2</sub>. HAP inevitably alters the band structure of TiO<sub>2</sub>, causing changes in light capture efficiency and expanding its spectral response range to the visible light area, hence increasing the photocatalytic activity of TiO<sub>2</sub>. This is similar to Sabah Taha's results.<sup>30</sup>

Mechanical properties are the key parameters of denture life.<sup>35</sup> The test results show that compared with pure PMMA, the tensile strength, bending strength, and bending modulus of PMMA first increase and then decrease with the additional proportion of TiO<sub>2</sub>-HAP complex. The mechanical properties of PMMA reach the best when the addition proportion is 1%wt. Several scholars have studied the inclusion of TiO<sub>2</sub>, HAP, and other nanoparticles into PMMA materials, revealing a general trend: the mechanical properties of PMMA materials initially increase in bending strength, bending modulus, and tensile strength, and then decrease.<sup>36-38</sup> According to the literature, the mechanism of nanoparticle-induced mechanical strength enhancement of PMMA materials involves the good dispersion of nanoparticles in the PMMA matrix, which increases the transverse strength and ductility and can achieve a significant increase in mechanical strength at a very low addition ratio.<sup>39</sup> The presence of complexes in the matrix restricts the movement of the matrix phase in the region around each particle, resulting in an overall increase in the modulus.<sup>40</sup> However, the increasing content of TiO<sub>2</sub>-HAP complexes will affect the dispersion of nanoparticle crystals in PMMA materials, resulting in agglomeration and the formation of stress concentration zones, thus weakening the mechanical properties of modified PMMA.<sup>41</sup> In the present experiment, analysis of the mechanical properties after testing provides a view consistent with previous studies.

Color change is a key aspect for aesthetic purposes, as PMMA-based materials are destined for use in clinical practice. The transmittance refers to the percentage of the light flux passing through the material and the incident light flux, which is the most important indicator to measure the transparency effect of the material.<sup>42</sup> The content and dispersion of TiO<sub>2</sub>-HAP in the PMMA matrix are the key factors to achieve high transmittance.<sup>43</sup> In this experiment, The transmittance of the sample

decreases with the increase of the addition proportion, which is consistent with the results reported in some studies that the addition of small particle fillers can lead to a significant decrease in the transmittance of the composite material, which can be attributed to the diffuse light transmission caused by multiple scattering of light in the material. In this experiment, the transmittance of the 1%wt group was 34.87%, which decreased less than that of the control group, only 7.22%. However, when the transmittance exceeded 1%wt, the transmittance dropped sharply, and the transmittance of the 1.5%wt group was only 23.11%. We can not compare the light transmission results of other studies because no previous studies were found to evaluate the light transmission of denture base materials. But from another perspective, a small reduction in light transmission may produce better clinical outcomes, and in clinical situations where prostheses with lower light transmission have greater color masking, preventing gray shading or color inconsistencies from the underlying metal frame in the prosthesis, achieving better aesthetic results.<sup>44</sup> Color variation was also evaluated. In all experimental groups, the 0.5%wt and 1%wt groups reported  $\Delta E$  values indicating visually perceptible color changes compared to the control group, unlike some other antimicrobials, such as nanosilver.<sup>45</sup>

The prepared modified PMMA showed no obvious cytotoxicity in cck8 and cell death tests, which was lacking in most previous studies.<sup>46,47</sup> TiO<sub>2</sub> and HAP are both biologically active chemicals that have been used in many clinical Settings and have proven biocompatibility.<sup>48,49</sup> Low cytotoxicity is an important condition for their clinical application. It can be inferred that when the addition of TiO<sub>2</sub>-HAP is limited to less than 2.0%wt, the biosafety of modified PMMA materials is still favorable.

In this experiment, the addition of TiO<sub>2</sub>-HAP reduces the contact angle of PMMA to less than that of the pure PMMA, which is consistent with the results reported in several studies that the contact angle of PMMA changes with the addition of nano-fillers.<sup>50</sup> Studies show that the addition of TiO<sub>2</sub> nanoparticles in PMMA can improve hydrophilicity and reduce the possibility of bacterial adhesion.<sup>51</sup> Some studies have tested the effect of contact angle on the adhesion of *Candida albicans* and found that contact angle significantly affects the adhesion of *Candida albicans* to PMMA. One of the main factors affecting the adhesion of *Candida albicans* is the surface hydrophilicity of the sample. With the increase of hydrophilicity, the formation of *Candida* biofilm will be inhibited.<sup>52</sup> Therefore, improving the hydrophilicity of the repaired body surface may be an effective way to reduce the adhesion of *Candida albicans*. In this study, with the increase of the addition of TiO<sub>2</sub>-HAP nanoparticles, the contact angle showed a decreasing trend. It can be seen that the addition of TiO<sub>2</sub>-HAP nanoparticles reduces the surface contact angle, increases the surface hydrophilicity, and reduces the adhesion of *Candida albicans*. Therefore, we infer that the addition of TiO<sub>2</sub>-HAP nanoparticles to PMMA can reduce bacterial adhesion and biofilm thickness.

Through the above experiments, we selected the 1%wt group to investigate its photodynamic antifungal activity under visible light. The experimental results showed that, combined with the light curing lamp, the TiO<sub>2</sub> group or TiO<sub>2</sub>-HAP group had obvious antifungal effects compared with the control group, This is consistent with wang's results.<sup>22</sup> Moreover, the antibacterial efficiency of the TiO<sub>2</sub>-HAP group was higher than that of the TiO<sub>2</sub> group, reaching 94%, indicating that the introduction of HAP as a photocatalytic antibacterial activity of TiO<sub>2</sub> increased. This may be attributed to the antibacterial activity of TiO<sub>2</sub>-HAP nanoparticles or their potential role in improving the hydrophilicity of PMMA. Electron microscopy shows that TiO<sub>2</sub>-HAP in PMMA under blue light exhibits antibacterial effects by disrupting the integrity of *Candida albicans*, which is consistent with the findings of Mohammadi S.<sup>53</sup> Under visible light excitation, TiO<sub>2</sub>-HAP can damage yeast cells through coenzyme A oxidation and lipid peroxidation by producing reactive oxygen species, destroy the integrity of *Candida albicans*, and lead to cell rupture. No *Candida albicans* bud tube or mycelium form was detected on the surface of the material, indicating that modified PMMA could inhibit the transition of *Candida albicans* from a yeast phenotype to a more virulent filamentous phenotype.<sup>54</sup>

In our study, the recommended proportion of TiO<sub>2</sub>-HAP nanoparticles incorporated into PMMA is 1%wt, which has excellent antifungal activity under visible light and stronger mechanical properties for clinical use. The optical properties are still in the clinically acceptable range, and the low toxicity of these nanoparticles to living cells compared to other types of nanomaterials ensures that they are the best choice for customized PMMA, but note that in practical clinical applications, K marek et al argue that photocatalytic antimicrobial therapy is generally considered to be a safer antimicrobial approach. Because it has no negative effects on oral tissue.<sup>55</sup> However, some studies have found that this therapy can produce pain and other side effects.<sup>56</sup> So the practical application of this study is to activate modified PMMA to inhibit bacteria in vitro, rather than in vivo, to minimize discomfort, damage, or other adverse effects that may occur when tissues are exposed to blue light.

The significance of the study is in the prevention and potential therapeutic effects of the modified PMMA denture base in threatening *Candida albicans* in elderly patients. These patients often wear dentures, that are poorly cleaned and are more likely to develop opportunistic infections. A simpler, safer, and more successful method is introduced, especially for the elderly, disabled, and hospitalized patients. It only needs to be activated under visible light to give full play to its efficient antibacterial ability, kill fungi on the surface of the base, and realize home care. However, we still need to verify the influence of excitation time on the antibacterial effect. Meanwhile, since the effective antibacterial performance of the material may weaken with time, it is also necessary to consider how long the antibacterial effect of modified PMMA can last in the future. To determine the exact mechanism of the interaction between light, photosensitizers, PMMA, and oral bacteria, as well as to test the antibacterial properties of this modified PMMA material against oral bacteria other than *Candida albicans*, more in vivo oral tests are needed.

## Conclusion

When only 1%wt TiO<sub>2</sub>-HAP was added to PMMA, the photocatalytic antimicrobial properties and mechanical properties of PMMA materials reached the best without causing significant changes in cytotoxicity and optical properties.

## Data Sharing Statement

This article has all the data that were created or evaluated during this investigation.

## Ethics Approval and Informed Consent

Informed consents were signed with the approval of the Ethics Committee of The Affiliated Stomatological Hospital, Southwest Medical University, Luzhou, China (permit number: 20220912003). All research studies have been performed in accordance with the principles stated in the Declaration of Helsinki.

## Funding

This work was supported by Luzhou Science and Technology Bureau (Grant number 2024RCM239), Sichuan Natural Science Foundation (2024NSFSC0566).

## Disclosure

The author(s) report no conflicts of interest in this work.

## References

1. Tyrovolas S, Koyanagi A, Panagiotakos DB, et al. Population prevalence of edentulism and its association with depression and self-rated health. *Sci Rep*. 2016;6(1):37083. doi:10.1038/srep37083
2. Douglass CW, Shih A, Ostry L. Will there be a need for complete dentures in the United States in 2020?; research support, non-U. Gov't S. *J Prosthetic Dent*. 2002;87(1):5–8. doi:10.1067/mp.2002.121203
3. Friel T, Waia S. Removable partial dentures for older adults. *Primary Dental J*. 2020;9:34–39. doi:10.1177/2050168420943435
4. Aldabib J, Ishak Z. Fracture toughness of poly (methyl methacrylate)/hydroxyapatite denture base composite: effect of planetary ball milling mixing time. *J Phys Sci*. 2021;32:103–116. doi:10.21315/jps2021.32.3.8
5. Diez-Pascual AM. PMMA-based nanocomposites for odontology applications: a state-of-the-art. Review. *Int J Mol Sci*. 2022;23(18):10288. doi:10.3390/ijms231810288
6. Zafar MS. Prosthodontic applications of polymethyl methacrylate (PMMA): an update. Review. *Polymers*. 2020;12(10):2299. doi:10.3390/polym12102299
7. Barbur I, Opris H, Colosi HA, et al. Improving the mechanical properties of orthodontic occlusal splints using nanoparticles: silver and zinc oxide. *Biomedicines*. 2023;11(7):1965. doi:10.3390/biomedicines11071965
8. Brown JL, Young T, McCloud E, et al. An In vitro evaluation of denture cleansing regimens against a polymicrobial denture biofilm model. *Antibiotics*. 2022;11(1):113. doi:10.3390/antibiotics11010113
9. Yarbrough A, Cooper L, Duquim I, Mendonça G, McGraw K, Stoner L. Evidence regarding the treatment of denture stomatitis. *J Prosthodont*. 2016;25(4):288–301. doi:10.1111/jopr.12454
10. Lima LFG, de Paula Castro V, Álvarez CMO, Ambrósio SR, Rodrigues MA, Pires RH. Assessing the efficacy of gutiferone E in photodynamic therapy for oral candidiasis. *J Photochem Photobiol B Biol*. 2024;250:112834. doi:10.1016/j.jphotobiol.2023.112834
11. Rai LS, Wijlick LV, Bougnoux ME, Bachellier-Bassi S, d'Enfert C. Regulators of commensal and pathogenic life-styles of an opportunistic fungus-*Candida albicans*. *Yeast*. 2021;38(4):243–250. doi:10.1002/yea.3550
12. Skupien JA, Valentini F, Boscato N, Pereira-Cenci T. Prevention and treatment of *Candida* colonization on denture liners: a systematic review. *J Prosthet Dent*. 2013;110(5):356–362. doi:10.1016/j.prosdent.2013.07.003



13. Fotovat F, Abbasi S, Nikanjam S, Alafchi B, Baghiat M. Effects of various disinfectants on surface roughness and color stability of thermoset and 3D-printed acrylic resin. *Eur J Trans Myol.* **2024**;34(1). doi:10.4081/ejtm.2024.11701
14. Tulbah HI. Anticandidal efficacy on polyimide based denture resin using photodynamic therapy, chemical and herbal disinfectants and their effect on surface roughness and hardness. *Photodiagn Photodyn Ther.* **2022**;39:102874. doi:10.1016/j.pdpdt.2022.102874
15. Hu Q, Li T, Yang J, Peng Y, Liu Q, Liu N. Efficacy of photodynamic therapy in the treatment of oral candidiasis: a systematic review and meta-analysis. *BMC Oral Health.* **2023**;23(1):802. doi:10.1186/s12903-023-03484-z
16. Zhou M, Zhang X, Quan Y, Tian Y, Chen J, Li L. Visible light-induced photocatalytic and antibacterial adhesion properties of superhydrophilic TiO<sub>2</sub> nanoparticles. *Sci Rep.* **2024**;14(1):7940. doi:10.1038/s41598-024-58660-0
17. Thakur N, Thakur N, Kumar A, et al. A critical review on the recent trends of photocatalytic, antibacterial, antioxidant and nanohybrid applications of anatase and rutile TiO<sub>2</sub> nanoparticles. *Sci Total Environ.* **2024**;914:169815. doi:10.1016/j.scitotenv.2023.169815
18. AlQahtani GM, AlSuhail HS, Alqater NK, et al. Polymethylmethacrylate denture base layering as a new approach for the addition of antifungal agents. *J Prosthodont.* **2023**;32(4):298–308. doi:10.1111/jopr.13561
19. Patel MP, Parmar VB, Rami DS, Rakesh Trivedi V, Rana DM, Bajanania DN. Comparative evaluation of the effect of microwave, 1% sodium hypochlorite, and sodium perborate disinfection on the color stability of two nanoparticle-reinforced heat-polymerized PMMA denture base resins: an in vitro study. *Cureus.* **2024**;16(8):e67350. doi:10.7759/cureus.67350
20. Gao R, Hao C, Xu L, et al. Near-infrared chiroptical activity titanium dioxide supraparticles with circularly polarized light induced antibacterial activity. *ACS Nano.* **2024**;18(1):641–651. doi:10.1021/acsnano.3c08791
21. Jouda NS, Fadhel Essa A. Preparation and study of the structural, physical and mechanical properties of hydroxyapatite nanocomposite. *Mater Today Proc.* **2021**;47:5999–6005. doi:10.1016/j.matpr.2021.04.550
22. Wang R, Jia C, Zheng N, et al. Effects of photodynamic therapy on Streptococcus mutans and enamel remineralization of multifunctional TiO (2)-HAP composite nanomaterials. *Photodiagn Photodyn Ther.* **2023**;42:103141. doi:10.1016/j.pdpdt.2022.103141
23. Li Y, Zhang D, Wan Z, Yang X, Cai Q. Dental resin composites with improved antibacterial and mineralization properties via incorporating zinc/strontium-doped hydroxyapatite as functional fillers. *Biomed Mat.* **2022**;17(4):045002. doi:10.1088/1748-605X/ac6b72
24. Mirković M, Filipović S, Kalijadis A, et al. Hydroxyapatite/TiO<sub>2</sub> nanomaterial with defined microstructural and good antimicrobial properties. *Antibiotics.* **2022**;11(5):592. doi:10.3390/antibiotics11050592
25. Takhtdar M, Azizimoghadam N, Kalantari MH, Mohaghegh MA-O. Effect of denture cleansers on color stability and surface roughness of denture bases fabricated from three different techniques: conventional heat-polymerizing, CAD/CAM additive, and CAD/CAM subtractive manufacturing. *Clin Exp Dental Res.* **2023**;9(5):840–850. doi:10.1002/cre2.763
26. Huang J, Xiong T, Zhang Z, Tan Y, Guo L. Inhibition of the receptor for advanced glycation inhibits lipopolysaccharide-mediated High mobility group protein B1 and Interleukin-6 synthesis in human gingival fibroblasts through the NF-κB signaling pathway. *Arch Oral Biol.* **2019**;105:81–87. doi:10.1016/j.archoralbio.2019.06.006
27. Delgado K, Quijada R, Palma R, Palza H. Polypropylene with embedded copper metal or copper oxide nanoparticles as a novel plastic antimicrobial agent. *Lett Appl Microbiol.* **2011**;53(1):50–54. doi:10.1111/j.1472-765X.2011.03069.x
28. Yu JC, Zhang L, Yu J. Direct sonochemical preparation and characterization of highly active mesoporous TiO<sub>2</sub> with a bicrystalline framework. *Chem Mater.* **2002**;14(11):4647–4653. doi:10.1021/cm0203924
29. Jie Y, Zhang Y, Wang Y, et al. Enhanced photocatalytic removal of NO over titania/hydroxyapatite (TiO<sub>2</sub>/HAp) composites with improved adsorption and charge mobility ability. *RSC Adv.* **2017**;7:24683–24689. doi:10.1039/C7RA02157G
30. Taha S, Begum S, Narwade VN, et al. Development of alcohol sensor using TiO<sub>2</sub>-Hydroxyapatite nano-composites. *Mater Chem Phys.* **2020**;240:122228. doi:10.1016/j.matchemphys.2019.122228
31. Ahmad I, Zou Y, Yan J, et al. Semiconductor photocatalysts: a critical review highlighting the various strategies to boost the photocatalytic performances for diverse applications. *Adv Colloid Interface Sci.* **2023**;311:102830. doi:10.1016/j.cis.2022.102830
32. Chai YD, Pang YL, Lim S, Chong WC, Lai CW, Abdullah AZ. Recent progress on tailoring the biomass-derived cellulose hybrid composite photocatalysts. *Polymers.* **2022**;14(23). doi:10.3390/polym14235244
33. Mariappan A, Pandi P, Rajeswarapalanichamy R, et al. Bandgap and visible-light-induced photocatalytic performance and dye degradation of silver doped HAp/TiO<sub>2</sub> nanocomposite by sol-gel method and its antimicrobial activity. *Environ Res.* **2022**;211:113079. doi:10.1016/j.envres.2022.113079
34. Keesmann I. Zur hydrothermalen Synthese von Brookit. *Z Anorg Allg Chem.* **1966**;346(1–2):30–43. doi:10.1002/zaac.19663460105
35. Balhaddad AA, Garcia IM, Mokeem L, Alsaifi R, Collares FM, Sampaio de Melo MA. Metal oxide nanoparticles and nanotubes: ultrasmall nanostructures to engineer antibacterial and improved dental adhesives and composites. *Bioengineering.* **2021**;8(10):146. doi:10.3390/bioengineering8100146
36. Aldabib J, Ishak Z. Effect of hydroxyapatite filler concentration on mechanical properties of poly (methyl methacrylate) denture base. *SN Appl Sci.* **2020**;2. doi:10.1007/s42452-020-2546-1.
37. Karci M, Demir N, Yazman S. Evaluation of flexural strength of different denture base materials reinforced with different nanoparticles. *J Prosthodont.* **2019**;28(5):572–579. doi:10.1111/jopr.12974
38. Shirkavand S, Moslehifard E. Effect of TiO<sub>2</sub> nanoparticles on tensile strength of dental acrylic resins. *J Dental Res Dental Clinics Dental Prospects.* **2014**;8(4):197–203. doi:10.5681/joddd.2014.036
39. Hata K, Ikeda H, Nagamatsu Y, Masaki C, Hosokawa R, Shimizu H. Dental poly(methyl methacrylate)-based resin containing a nanoporous silica filler. *J funct biomat.* **2022**;13(1):32. doi:10.3390/jfb13010032
40. Kang I-G, Cheonil P, Lee H, Kim HJ, Lee S-M. Hydroxyapatite microspheres as an additive to enhance radiopacity, biocompatibility, and osteoconductivity of poly(methyl methacrylate) bone cement. *Materials.* **2018**;11:258. doi:10.3390/ma11020258
41. An J, Ding N, Zhang Z. Mechanical and antibacterial properties of polymethyl methacrylate modified with zinc dimethacrylate. *J Prosthet Dent.* **2022**;128(1):100.e1–100.e8. doi:10.1016/j.prosdent.2022.04.029
42. Busato S, Perevedentsev A. *A Simple, Versatile Imaging Technique for Quantifying the Haze of materials*; **2017**. doi:10.2417/spepro.006936
43. Arikawa H, Kanie T, Fujii K, Takahashi H, Ban S. Effect of filler properties in composite resins on light transmittance characteristics and Color. *Dental Mat J.* **2007**;26(1):38–44. doi:10.4012/dmj.26.38

44. Altonbary GY, Emera RMK. Patient satisfaction and masticatory performance of zirconia bar compared to cobalt chromium bar retaining mandibular implant overdenture: a crossover study. *J Oral Rehab.* **2021**;48(7):827–835. doi:10.1111/joor.13164
45. Nam KY. Chapter 12 - Characterization and antifungal activity of the modified PMMA denture base acrylic: nanocomposites impregnated with gold, platinum, and silver nanoparticles. In: Grumezescu AM, editor. *Nanobiomaterials in Dentistry*. William Andrew Publishing; **2016**:309–336.
46. De Matteis V, Cascione M, Toma CC, et al. Silver nanoparticles addition in poly(methyl methacrylate) dental matrix: topographic and antimycotic studies. *Int J Mol Sci.* **2019**;20(19):4691. doi:10.3390/ijms20194691
47. Vikram S, Chander G. Effect of zinc oxide nanoparticles on the flexural strength of polymethylmethacrylate denture base resin. *Eur Oral Res.* **2020**;54:31–35. doi:10.26650/eor.20200063
48. Shang S, Zhuang K, Chen J, Zhang M, Jiang S, Li W. A bioactive composite hydrogel dressing that promotes healing of both acute and chronic diabetic skin wounds. *Bioact Mater.* **2024**;34:298–310. doi:10.1016/j.bioactmat.2023.12.026
49. Wang B, Wu Z, Wang S, et al. Mg/Cu-doped TiO<sub>2</sub> nanotube array: a novel dual-function system with self-antibacterial activity and excellent cell compatibility. *Mater Sci Eng C Mater Biol Appl.* **2021**;128:112322. doi:10.1016/j.msec.2021.112322
50. Marić I, Zore A, Rojko F, et al. Antifungal effect of polymethyl methacrylate resin base with embedded au nanoparticles. *Nanomaterials.* **2023**;13(14):2128. doi:10.3390/nano13142128
51. Cascione M, De Matteis V, Pellegrino P, et al. Improvement of PMMA dental matrix performance by addition of titanium dioxide nanoparticles and clay nanotubes. *Nanomaterials.* **2021**;11(8):2027. doi:10.3390/nano11082027
52. Lazarin AA, Machado AL, Zamperini CA, Wady AF, Spolidorio DM, Vergani CE. Effect of experimental photopolymerized coatings on the hydrophobicity of a denture base acrylic resin and on *Candida albicans* adhesion. *Arch Oral Biol.* **2013**;58(1):1–9. doi:10.1016/j.archoralbio.2012.10.005
53. Mohammadi S, Mohammadi P, Hosseinkhani S, Shipour R. Antifungal activity of TiO<sub>2</sub> nanoparticles and EDTA on *Candida albicans* biofilms. *Infect Epidemiol Med.* **2013**;1:33–38.
54. Samaranayake YH, Cheung BP, Yau JY, Yeung SK, Samaranayake LP. Human serum promotes *Candida albicans* biofilm growth and virulence gene expression on silicone biomaterial. *PLoS One.* **2013**;8(5):e62902. doi:10.1371/journal.pone.0062902
55. Kömerik N, Curnow A, MacRobert AJ, Hopper C, Speight PM, Wilson M. Fluorescence biodistribution and photosensitising activity of toluidine blue o on rat buccal mucosa. *Lasers Med Sci.* **2002**;17(2):86–92. doi:10.1007/s101030200015
56. Borgia F, Giuffrida R, Caradonna E, Vaccaro M, Guarneri F, Cannavò SP. Early and late onset side effects of photodynamic therapy. *Biomedicines.* **2018**;6(1):12. doi:10.3390/biomedicines6010012

International Journal of Nanomedicine

Publish your work in this journal

The International Journal of Nanomedicine is an international, peer-reviewed journal focusing on the application of nanotechnology in diagnostics, therapeutics, and drug delivery systems throughout the biomedical field. This journal is indexed on PubMed Central, MedLine, CAS, SciSearch®, Current Contents®/Clinical Medicine, Journal Citation Reports/Science Edition, EMBase, Scopus and the Elsevier Bibliographic databases. The manuscript management system is completely online and includes a very quick and fair peer-review system, which is all easy to use. Visit <http://www.dovepress.com/testimonials.php> to read real quotes from published authors.

Submit your manuscript here: <https://www.dovepress.com/international-journal-of-nanomedicine-journal>

**Dovepress**  
Taylor & Francis Group